

First time-series optical photometry from Antarctica

sIRAIT monitoring of the RS CVn binary V841 Centauri and the δ -Scuti star V1034 Centauri

K. G. Strassmeier¹, R. Briguglio^{2,3}, T. Granzer¹, G. Tosti², I. DiVarano¹, I. Savanov¹, M. Bagaglia², S. Castellini², A. Mancini², G. Nucciarelli², O. Straniero⁴, E. Distefano⁵, S. Messina⁵ and G. Cutispoto⁵

¹ Astrophysical Institute Potsdam (AIP), An der Sternwarte 16, D-14482 Potsdam, Germany;

e-mail: kstrassmeier@aip.de, e-mail: tgranzer@aip.de, e-mail: idivarano@aip.de, e-mail: isavanov@rambler.ru

² Dipartimento di Fisica, Università di Perugia, Via A. Pascoli, I-06100 Perugia, Italy;

e-mail: runa@fisica.unipg.it, e-mail: gino.tosti@fisica.unipg.it

³ Concordia, Dome C, Antarctica; <http://www.concordiabase.eu>

⁴ INAF Osservatorio Teramo, Via Mentore Maggini, I-64100 Teramo, Italy

⁵ INAF - Catania Astrophysical Observatory, via S. Sofia 78, I-95123 Catania, Italy;

e-mail: sme@oact.inaf.it, e-mail: gcutispoto@oact.inaf.it, e-mail: edistefano@oact.inaf.it

Received ... ; accepted ...

ABSTRACT

Context. Beating the Earth’s day-night cycle is mandatory for long and continuous time-series photometry and had been achieved with either large ground-based networks of observatories at different geographic longitudes or when conducted from space. A third possibility is offered by a polar location with astronomically-qualified site characteristics.

Aims. In this paper, we present the first scientific stellar time-series optical photometry from Dome C in Antarctica and analyze approximately 13,000 CCD frames taken in July 2007.

Methods. The optical pilot telescope of the “International Robotic Antarctic Infrared Telescope”, named “small IRAIT” (sIRAIT), and its *UBVRI* CCD photometer were used in *BVR* for a continuous 243 hours (10.15 days) with a duty cycle of 98% and a cadence of 155 sec. The prime targets were the chromospherically active, spotted binary star V841 Cen and the non-radially pulsating δ -Scuti star V1034 Cen.

Results. We confirm the known 0.2-day fundamental period of V1034 Cen and found a total of 23 further periods between 2.2 hours and 3.5 days. V841 Cen’s *V* amplitude due to spots appeared to be at a record high of $0^m.4$ in *V* in July 2007. We present a spot-model analysis with a light-curve inversion technique and found the star with a spot filling factor of 44% of the visible hemisphere, among the highest ever measured values for active stars, and a temperature difference photosphere minus spot of 750 ± 100 K. Its odd-numbered (for a single site) rotation period was determined with a higher precision than before (5.8854 ± 0.0026 days) despite the comparably short data set. The rms scatter from a 2.4-hour data subset was 3 mmag in *V* and 4.2 mmag in *R*. The differential data quality is 3–4 times better than with the 25cm Fairborn Automatic Photoelectric Telescope in southern Arizona and is likely due to the exceptionally low scintillation noise at Dome C.

Conclusions. We conclude that high-precision CCD photometry with exceptional time coverage and cadence can be obtained at Dome C in Antarctica and be successfully used for time-series astrophysics.

Key words. stars: spots – stars: variables: general – stars: activity – stars: oscillations – stars: individual: V841 Cen – stars: individual: V1034 Cen

1. Introduction

Time-series photometry is a powerful tool to understand cosmic variabilities and their many underlying physical mechanisms, from Gamma Ray Bursts to the non-radial oscillations of our Sun. World-wide networks around the globe were organized to bypass the Earth’s day-night cycle, e.g. by the “Global Oscillation Network Group” (Harvey et al. 1996), the “Whole Earth Telescope” (Nather et al. 1990) or the “Multi Site Continuous Spectroscopy” campaigns (Catala et al. 1993), just to name a few. Despite their tremendous success such networks must cope with the many different site characteristics, the individual weather patterns and, most importantly, with the different instru-

ment/detector combinations and the respective calibration issues. An alternative to such networks is a single polar site.

The French-Italian Antarctic station *Concordia* at Dome C at a height of 3200m on the east Antarctic plateau is currently, besides the U.S. South Pole station, the only plateau station populated over winter (=night). In principle, it thus enables astronomical observations comparable to regular observatories at temperate sites. Dome C had received world-wide attention from the night-time astronomical community when it became known that the seeing conditions on the east Antarctic plateau are likely the best on the entire planet with a median seeing of $0.3''$ and occasionally even below $0.1''$ at a height of approximately 30m above ground (Lawrence et al. 2004, Agabi et al. 2006).

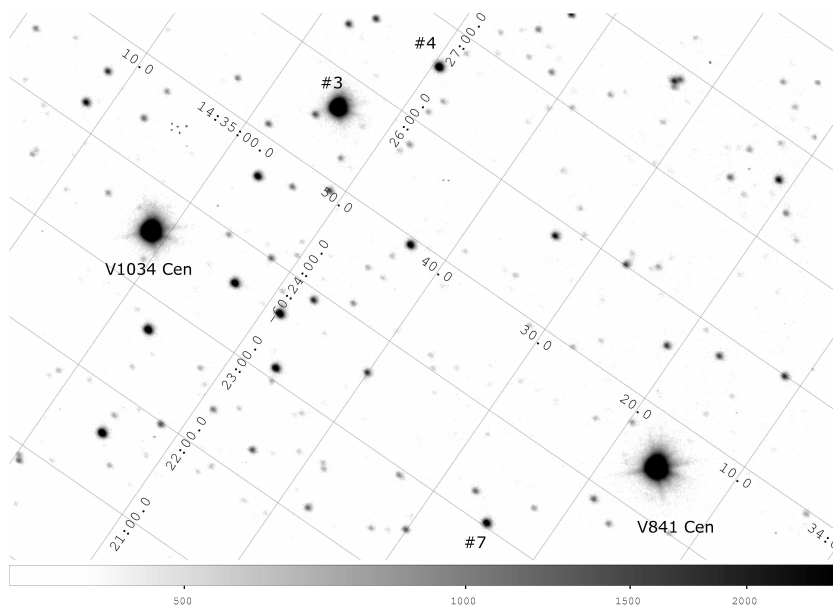


Fig. 1. Identification of stars in the CCD FOV ($8' \times 5.3'$). The three bright stars are our primary targets V841 Cen (right, $V=8^m.5$) and V1034 Cen (left) and the comparison star CD-59°5309 (top). The comparison star and stars #4 and #7 were identified as variable (see Table 1). The image shown is a composite of 20 individual R-band frames, each a 40-sec integration. The coordinates are for equinox 2000.0. The faintest stars are 16th magnitude.

Science cases that require continuous high-precision photometry uniquely benefit from the absent 24-hour day-night cycle and the consequently stable atmosphere in general. For example, δ Scuti stars are known to have a complex surface oscillation spectrum involving many modes and frequencies. The detection of patterns of closely-spaced peaks in different modes enables the determination of the internal stellar structure. The essential observational restriction is the frequency resolution, which is proportional to the length of the photometric time series. It sets limits to the mode identification and thus their unique interpretation. Another example are spotted stars. Magnetic spots, like those on the Sun, are tracers of the internal dynamo activity. Spot size and temperature are related to the magnetic flux that the emerging flux tube transported up from the interior. However, surface velocity fields like differential rotation affect the magnetic field (and vice versa) so that spots are likely only indirectly linked to the dynamo. Observing the migration behavior of starspots from one stellar rotation to the other, however, may constrain some global properties of the dynamo.

Additionally, optical photometry of bright stars may be brought down to the photon-noise level because atmospheric scintillation noise appears to be a factor 3.6 smaller (Kenyon et al. 2006) than at the best temperate sites. The detailed issues for optical photometry from Dome C were highlighted by several authors, most recently by Vernin et al. (2007), Strassmeier (2007) and Kenyon et al. (2006). We also note the early attempts and experiences from the South Pole’s “Vulcan-South” experiment¹ that, unfortunately, suffered from the comparable harsh winds at the South Pole.

A continuous 1500-hour night opens up a new window for science cases like the search for extra-solar planets (e.g. Pont & Bouchy 2005, Deeg et al. 2005), for asteroseismology (e.g. Fossat 2005) and for stellar rotation and activity studies (e.g. Strassmeier & Oláh 2004). Several astronomical experiments are now planned for Dome C (for a compilation see Strassmeier et al. 2007a). Among these pilot experiments is a small 25-cm optical precursor telescope

for the 80-cm infrared telescope IRAIT (Tosti et al. 2006) and the 2×60 cm Schmidt-telescope ICE-T (Strassmeier et al. 2007b). sIRAIT was designed to experience the expected same difficulties in the same operative conditions foreseen for the larger projects with the goal of performing a period of full tests on a smaller scale.

In the current paper, we present and analyze the first data from sIRAIT from one CCD field obtained in July during winter 2007. Our primary target, V841 Cen, is a spotted, very active RS CVn binary with occasional flares and with an orbital period so close to a multiple of a day (5.998 days) that time-series data from a single, non-polar site severely undersamples its light curve. Our secondary target is the δ -Scuti star V1034 Cen, a non-radially pulsating star in the lower part of the instability strip with a (likely) fundamental period of ≈ 0.2 days.

2. Instrumental set up and observations

2.1. sIRAIT

sIRAIT is a 25-cm, effective f/12 Cassegrain optical telescope on a parallactic mount located near the *Concordia* station in the open field without a protection building ($75^\circ 06' 04''$ S, $123^\circ 20' 52''$ E, 3233m WGS84). Its CCD photometer is located approximately 1m above the ground. The telescope was designed by the IRAIT team at the University of Perugia, Italy (Tosti et al. 2006) and built by the *Marcon* telescope factory of San Donà di Piave, Italy, equipped with electronics and installed at Dome C by one of the coauthors (R. Briguglio). It is equipped with a guiding refractor placed along the optical tube and moved by two extreme-environment stepper motors, originally designed for vacuum and suitable for very low temperatures.

The focal-plane unit contains the CCD camera, the filter wheel, two heaters, two fans, thermo-couples and Pt100 probes, the mirror adjustment device and other electronics. It is insulated by a thin layer of foam and it is internally heated by two resistance heaters. The temperature achieved is constant to within 0.3°C in the inner CCD box, and $5^\circ \pm 2^\circ\text{C}$ in the motor-drivers box. During acquisition the CCD temperature is set at -28°C . The pho-

¹ <http://www.polartransits.org>

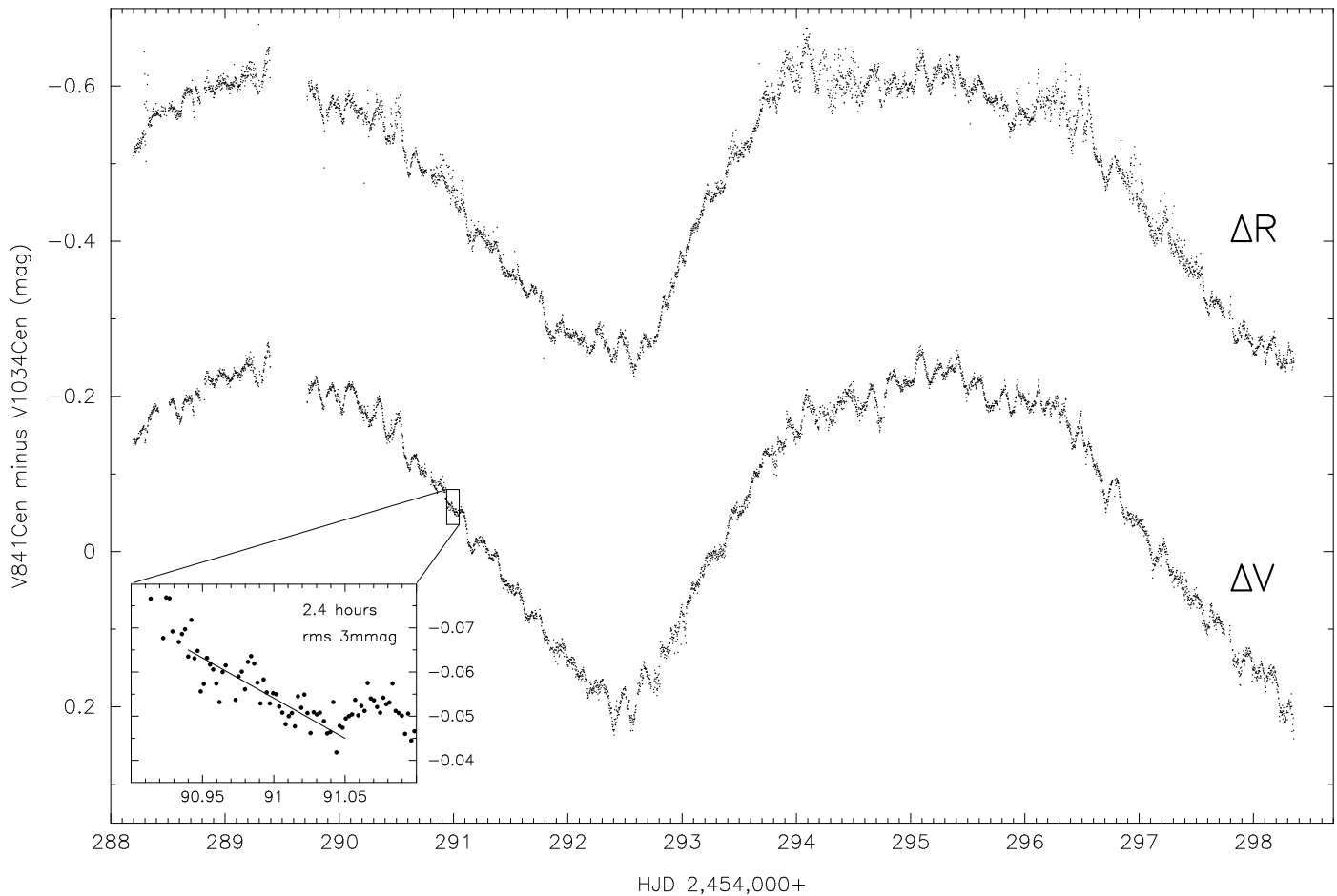


Fig. 2. Ten-day continuous differential VR photometry of V841 Cen minus V1034 Cen. Note that the long-period variation with an amplitude of 0^m4 in V is due to spots rotating in and out of view on V841 Cen while the short-period variations with an amplitude of $\approx 0^m02$ are due to non-radial pulsations of V1034 Cen. The insert shows a fraction of V data that is nearly free of intrinsic short-term stellar variations. The residuals from a simple linear fit to a 2.4-hour subset suggest a rms scatter of just 3 mmag in V (4.2 mmag in R). For such a long duration, this is 3–4 times better than an equally sized telescope at a temperate site.

tometer is a commercial MaxCam CCD camera by Finger Lakes Instruments (FLI). It is equipped with panchromatic Johnson $UBVRI$ filters and a focusing device. A Kodak KAF-0402ME CCD with 768×512 $9 \mu\text{m}$ pixels provides a field-of-view (FOV) of $8' \times 5.3'$ with an image scale of $0.65''/\text{pixel}$. Its quantum efficiency is given by the manufacturer to 55% in B , 80% in V and 60% in R . The full-well capacity is reached at 100,000 electrons and the FLI controller allows a read-out-noise of 15 electrons at nominal read-out speed of ≈ 500 kbit/s at a gain of $10 \mu\text{V}/e^-$. From the flat-fields, we estimate a gain of $2.1e^-/\text{ADU}$ and a read-out noise of $12.8e^-$, according to the procedure summarized in Janesick (1997). The typical point-spread-function (PSF) measured from a V -band frame is a Gaussian with a full-width at half maximum of 7.1 pixels ($4.6''$) for a star with $V=9^m0$, 30-sec exposure, 16,000 ADU at peak and $S/N=12:1$. Such an over-sampled PSF minimizes many practical problems, e.g., the contribution of partial pixels at the PSF's edge, the PSF changes due to e.g. focus changes, tracking and guiding errors, wind shake, or differential refraction but at the expense of increased crowding by background stars.

2.2. Acquisition and reduction of photometric data

Both primary targets are in the same FOV of the CCD, itself centered at $\alpha = 14^h34^m40^s$ and $\delta = -60^\circ25'$ (2000.0) (Fig. 1). The telescope acquired and tracked this FOV semi-automatically for a total of 243 continuous and consecutive hours (10.15 days) with only a single 5.8-hour interruption (Fig. 2). Observations started at HJD 2,454,288.199. A total of 13,000 CCD frames were acquired. Note that the data were taken July 6–16, 2007, but the raw data arrived in Europe only by the end of January 2008 when the winter-over crew was able to leave the station.

A sequence of observations consisted of consecutive BVR frames with 60s, 50s, and 40s integration times, respectively, typically allowing for approximately 20 images per hour per filter with an average time resolution of 155 sec. A daily ≈ 20 –30 minutes were needed for telescope derotation to unwind its electric cabling but is barely noticeable in Fig. 2. A single 5.8-hour gap occurred on the second day when the field was lost due to a tracking error. The counts per pixel were on average half of the full-well capacity of the CCD. The ratio of the sum of all background corrected pixels within the aperture (approximately 20,000 pixels) to the standard deviation of the background gives

Table 1. Log of three other variable stars in the CCD FOV.

ID	NOMAD	α (in deg) δ (in deg)	V σ_V	R σ_R	Notes
3	0295-0641140	218.72680 -60.4277	9.57 0.028	9.13 0.028	P=3.0d,1.5d
4	0295-0640999	218.70627 -60.4432	12.82 0.051	12.89 0.16	no clear P
7	0296-0615795	218.60366 -60.3841	13.14 0.24	13.17 0.25	no clear P

Note: ID is the internal identification according to Fig. 1. ID=3 is the original comparison star CD-59°5309. NOMAD is the NOMAD catalog number (Zacharias et al. 2005). α and δ are for equinox 2000.0. V and R are their average magnitudes in the Johnson system, and σ_V and σ_R the standard deviations from the mean in the V and R bandpasses in magnitudes.

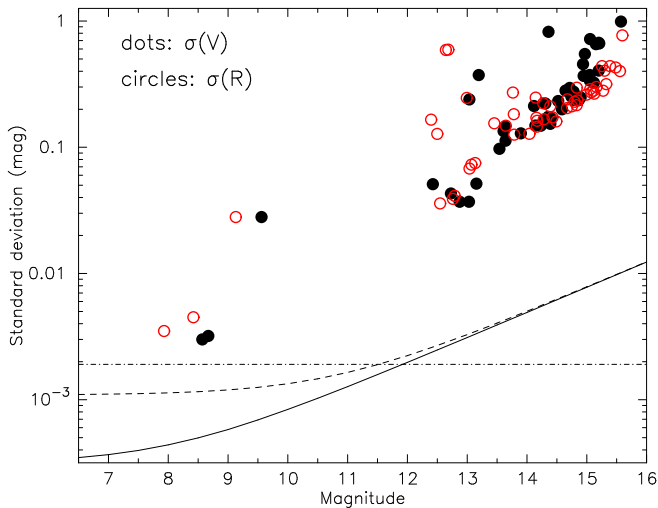


Fig. 3. V and R -band scatter diagram for an exposure time of 50 sec (V) and 40 sec (R). The precision for the two target stars ($V \approx 8^m5$) was 3 mmag in V and 4.2 mmag in R . The lines indicate the sum of the photon and scintillation noise for a temperate site (dashed line) and for Dome C (full line). The horizontal dash-dotted line is an *estimate* of the convolved sky plus detector limit for sIRAiT.

a peak S/N ratio in V and R of 15,000:1 for V841 Cen ($V=8^m5$). We did not correct for cosmic-ray hits as these were rather seldom and did not affect the photometry.

During the 10 days of acquisition the weather was very stable and good, almost no wind, temperature around $-72^\circ \pm 2^\circ\text{C}$. Ground-layer seeing varied between $2.8''$ and an exceptional $5\text{--}6''$. The few data from the latter periods had internal deviations larger than 25 mmag and were rejected from the analysis (a total of ≈ 20 frames out of 13,000). A simple linear fit to a 2.4-hour long V and R data subset shows a standard deviation of 3.0 and 4.2 mmag, respectively. We consider these as upper limits because the selected data-subset may not be free of intrinsic variability (see insert of Fig. 2).

Calibration frames were obtained three days after the science observations and consisted of 20 twilight flat fields in $BVRI$ and series of biases. Flat fields were acquired from horizon pointing during “midday” when the Sun was still below the horizon but provided enough light for exposures.

Exposures of 30s, 20s, and 10s for BVR , respectively resulted on average in 20,000 counts. A data-cube fit to all 20 flat-field frames was performed to obtain a master flat. Dark frames were taken occasionally during the cable-derotation times and sum up to 18, 25, and 26 frames for B , V , and R , respectively.

Twenty-five standard stars from Landolt (2007; and references therein) were observed ten times each on a clear night on September 10th, 2007 at the end of the Antarctic night. The air mass range was between 2–3 and thus unfortunately always higher than for our science field. Large air-mass variations are impossible to obtain at Dome C because of its high geographic latitude. Images were acquired in $UBVRI$ but U suffered from very poor S/N and was discarded. Even B had comparably large scatter. Extinction coefficients of 0^m278 , 0^m179 , 0^m064 , and 0^m081 for B , V , R and I , respectively, were obtained from linear fits to the instrumental magnitudes versus air mass and then used to transform to the standard Johnson system (Briguglio 2008).

The designated comparison star was CD-59°5309. *Simbad*² lists it as a B-star with $V=9^m50$, $B - V=+0^m74$ and $U - B=-0^m27$ as its best-quality UBV values from Schild et al. (1983). Our data show it to be a low-amplitude variable star with $V=9^m57$, a 1σ scatter of 0^m028 , and $V - R=0^m44$. To increase its S/N ratio, we summed up once three and once ten consecutive V frames and then performed a period analysis on them. However, the noise in the summed 10-frame light curve appeared sometimes comparable to the individual frames. We attribute this to the jitter from tracking errors which sometimes even includes jumps. Nevertheless, both data sets revealed periods of 3.04 days and 1.54 days as the strongest peaks (both in a Scargle and a CLEAN application; see Sect. 4.1) but with rather low amplitudes comparable to the scatter of the data. Two more periods of 5.57 and 0.983 days appear significant but have even lower amplitudes while 6 more periods are possibly in the data but are judged unreliable due to the large amplitude of the noise. The residuals from a least-squares fit with all four periods is 0.05 mag. We conclude that the star is likely a non-radially pulsating B star with a fundamental period of either 3.0 or 1.5 days.

The CCD FOV contains another 60 stars that we were able to identify in NOMAD (Zacharias et al. 2005) with V magnitudes between $12^m4\text{--}15^m7$. None of these are identified in *Simbad* though. Two stars are possibly variable objects due to their higher-than-expected standard deviation and are listed in Table 1. No clear periods were found for either.

We employed the ARCO software package for CCD data reduction and analysis as described in Distefano et al. (2007). Standard CCD frame reduction consisted of bias and dark subtraction and flat-field division. We use the SExtractor (Bertin & Arnouts 1996) software to match stars detected in different CCD frames, select the best candidates for building an ensemble of comparison stars and identify the parameters that optimize the photometry of each star and minimize the scatter of light curves due to statistical fluctuations. Aperture photometry with an optimized aperture is then applied to all selected candidates between $R=7^m9$ and 15^m7 . Fig. 3 shows the scatter plot for V and R from a three-comparison star ensemble solution. We note that some stars were located so close to the

² <http://simbad.u-strasbg.fr/simbad/>

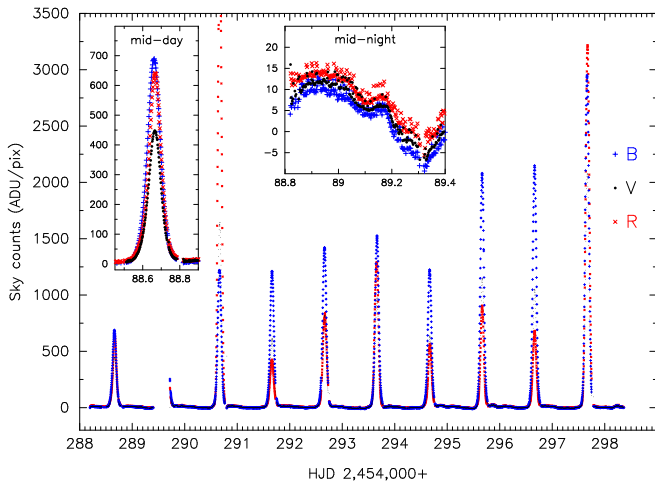


Fig. 4. Average background counts in *BVR* for the ten days of our observations. The inserts show an example of the counts during midday (left) and midnight (right), respectively. *BVR* is indicated with different plot symbols (pluses *B*, dots *V*, crosses *R*).

edge of the FOV that they were sometimes not identified by the photometry package which then resulted in artificially high residuals. These stars are not plotted in Fig. 3. An eye-ball fit to the lower envelope from ≈ 50 stars suggests a photometric precision of sIRAIT for the range 12^m5 to 15^m5 of 0^m04 at 12^m5 and 0^m4 at 15^m5 . For the very bright targets the precision is approximately 2.5 mmag above the expected scintillation-noise limit of 0.5 mmag (the full line in Fig. 3) while the faint stars are basically instrumental-noise limited (for a detailed discussion see Newberry 1991).

An estimate of the Dome-C sky brightness is obtained by using the background counts given by SExtractor on the dark-subtracted input frames (Fig. 4). We discarded all frames affected by twilight, i.e. during fractional JD of 0.5 to 0.85 as seen in Fig. 4. Note that moonlight did not contaminate our frames as we had waning moon. The maximum height of the moon above the horizon was 6° during the first night and 4° during the second night, after that it was continuously below the horizon reaching new moon two days before the end of our campaign. The remaining frames showed average background count rates of 2.99, 4.65, and 6.83 ADU/pix in *B*, *V*, and *R*, respectively, at a rms of around 6.5 ADU. Converting these to sky brightness per square-arcseconds yields magnitudes of 20^m77 , 20^m36 , 19^m90 in *B*, *V*, and *R*, respectively. We estimate that these values are good to within only $\approx 0^m1$. Examples are shown in the inserts of Fig. 4. Our *V* value is possibly significantly brighter than the GATTINI-SBC estimate of ≈ 21 Vmag/arcsec² converted from a Sloan *g* filter (Moore et al. 2007). Surprisingly, the background counts at midday varied by as much as a factor of four in *V* and *B*, and up to a factor of seven in *R* which may have resulted from illuminated high clouds. The ten-day rms at midnight was rather stable though and converts to a sky plus detector limit of 1.88 mmag in *V*. This is shown in Fig. 3 as a straight line.

2.3. Problems encountered

A spatially non-uniform gain of the CCD, dependent also on count-rate and time, did not allow the use of the original

comparison star for high-precision differential photometry. This behavior was not noticed in pre-shipment CCD tests and is likely due to the controller or the environment in which it has been working in Antarctica. However, the *B* bandpass was irreparably affected by this due to its already low count rates and we did not use it for further analysis.

Photometry with the full ensemble solution with 20 comparison stars resulted in more than twice the scatter for the two main targets than with respect to the differential magnitudes of the two bright stars themselves. The selection of the three next brightest and closest stars to V841 Cen as comparison stars resulted in a better but still more scattered light curve. Notice that all these bona-fide comparison stars are at least four magnitudes fainter than our two target stars, and the differential magnitudes are accordingly noisier. We bypassed this, and the gain problem, by using the δ -Scuti star V1034 Cen as the comparison star for V841 Cen (and vice versa) because it is the only star in the FOV with almost identical count rates.

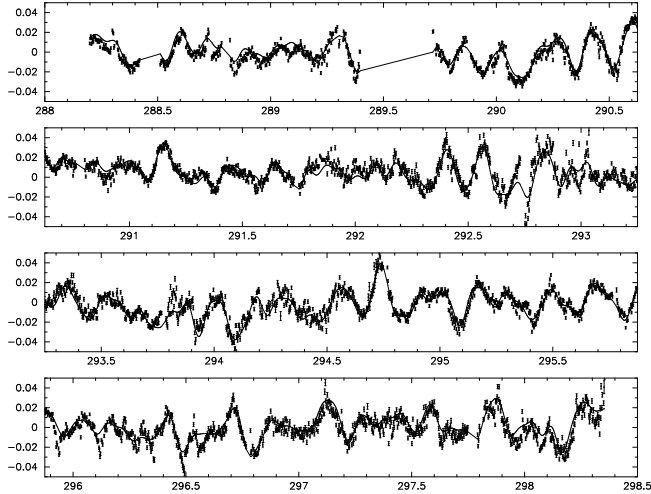
Another problem occurred when the optics were cleaned twice during the night (at HJD 2,454,292.68 and 93.71). Although technically not related with it, it likely caused another CCD controller (or USB connection) problem due to unwanted interference. On both occasions it had suddenly decreased the count rate for V841 Cen, but increased the count rate for V1034 Cen (on the same exposure). Both count rates then exponentially resettled to the previous (expected) count rates within ≈ 10 hours. We have no ready explanation for this but approximated the resettling trend with an exponential fit to the (differential) data and removed it. This introduced an extra scatter of ≈ 1 mmag during these 10 hours so that the standard deviation during these hours was more like $\sqrt{3^2 + 1^2} \approx 3.2$ mmag.

Next, we noticed that the telescope had severe pointing and tracking errors that accumulated during the run. Repositioning was done manually after approximately an hour or so. A scatter plot of the central coordinates of all, e.g., *V* frames shows an elongated distribution with a peak-to-peak range of $100''$ in both declination and right ascension. This means that the FOV usable for continuous photometry is just the minimum wrapped-in field from all individual pointings. With a CCD FOV of $8' \times 5.3'$ the range of $\pm 50''$ is a significant restriction. This probably impacted on the photometric precision because the photometric aperture did not always enclose exactly the same pixels.

3. The primary target stars

3.1. V841 Cen = HD127535

V841 Cen ($\alpha = 14^h34^m16^s$, $\delta = -60^\circ24'27''$, 2000.0, $V=8^m5$) is a rapidly rotating, single-lined spectroscopic binary with an active K1 subgiant as the primary component (Collier 1982a). The star exhibits strong CaII H&K and H α emission (Houk & Cowley 1975, Weiler & Stencel 1979). It shows high X-ray flux in the ROSAT 0.1–2.4 keV energy range (Dempsey et al. 1993) and in the EUV (Mitrou et al. 1997), and also very high radio-flux densities (Slee & Stewart 1989). Its lithium abundance of $\log n=0.77$ (Barrado y Navascués et al. 1998, but see also Randich et al. 1993 who obtained a significantly higher value) suggests a comparably young system. Randich et al. (1993) determined a $v \sin i$ of 33 ± 2 km s⁻¹ while De Medeiros et al. (1997) obtained 10 ± 1 km s⁻¹ from CORAVEL tracings.

a) V1034 Cen *V*-light curve

b) V1034 Cen periodogram

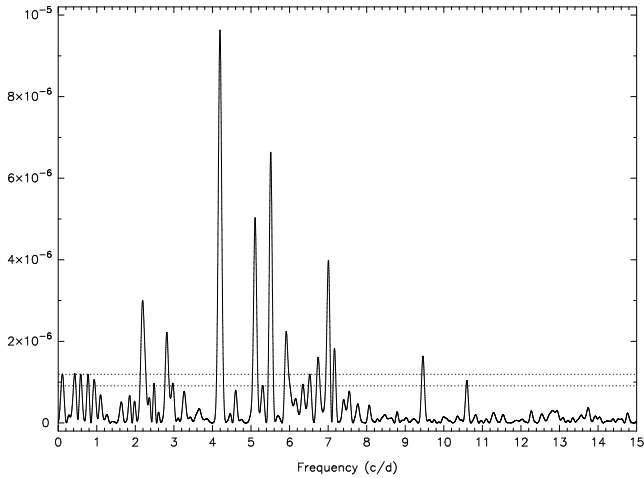


Fig. 5. **a** *V*-light curve of V1034 Cen after reconstructing and subtracting the variation of V841 Cen. Time is in fractional Julian Date as in Fig. 2. Error bars are $\pm 1\sigma$. The line is the least-squares fit with the frequencies in Table 2. **b** Period determination from a rectified CLEAN periodogram. The two horizontal lines indicate a false alarm probability of 10^{-6} (lower line) and 10^{-9} (upper line), respectively. A total of 20 periods between 2.2 hours and 3.5 days appear above the 10^{-6} FAP. Note the complete absence of the one-day period and its aliases.

The orbit is circular with a period of 5.998 days (Collier 1982a), while the photometric (= rotational) period of the K1 subgiant was given by Cutispoto (1990) to be 5.929 ± 0.024 days. Thus, the orbital motion and the stellar rotation are bound but not quite exactly synchronous and/or the subgiant’s surface is differentially rotating.

Previous photometry of V841 Cen was presented by Collier (1982b) from 1980–81, by Innis et al. (1998) from 1981, by Udalski & Geyer (1984) from 1984, by Bopp et al. (1986) from 1985, by Mekkadon & Geyer (1988) from April 1987, by Cutispoto (1990) from February 1987, by Cutispoto (1993) from 1989, by Cutispoto (1996) from Feb.-March 1990, by Cutispoto (1998a) from March 1991, by Cutispoto (1998b) from February 1992, by Strassmeier

Table 2. Period identifications for the δ Sct-star V1034 Cen.

No	Frequency (cycle/d)	Period (days)	Amplitude (mmag)	Notes
1	4.200	0.238	12.04	fundamental
2	5.514	0.181	9.91	stable
3	0.145	6.904	9.75	uncertain
4	0.461	2.169	9.71	uncertain
5	2.485	0.402	9.33	
6	5.107	0.196	8.90	stable
7	7.011	0.143	8.14	stable
8	0.766	1.304	7.80	uncertain
9	0.286	3.492	7.35	uncertain
10	2.192	0.456	6.87	
11	5.909	0.169	6.20	stable
12	6.738	0.148	5.94	stable
13	2.404	0.416	5.80	
14	7.161	0.140	5.78	stable
15	2.552	0.392	5.68	
16	9.462	0.106	5.09	stable
17	2.795	0.358	5.04	
18	2.941	0.340	5.02	
19	4.167	0.240	4.92	
20	6.509	0.154	4.41	
21	6.353	0.157	4.37	
22	10.600	0.094	4.11	stable
23	6.026	0.166	4.10	
24	5.294	0.189	4.04	

Note: The amplitude is the peak-to-valley *V* amplitude in milli-mag. Frequencies no. 11–24 are formally below the 1σ quality of the fit but are identified in the periodogram analysis in Fig. 5b. A “Stable” flag means that a frequency is mostly independent of other frequencies, “uncertain” means that the frequency is likely influenced by the length of the data set.

et al. (1994) from June–July 1994 and, most recently, by Innis & Coates (2008). At one occasion, Cutispoto (1998a) detected a flare lasting at least one day. V841 Cen is listed as star number CABS118 in the “Catalog of Chromospherically Active Binary Stars” (Strassmeier et al. 1993).

3.2. V1034 Cen = HD127695

V1034 Cen ($\alpha = 14^h 35^m 01^s$, $\delta = -60^\circ 23' 32''$, 2000.0, $V=8^m 7$) is an A9IV δ -Sct star with a period of 0.235 days and a full amplitude of $0^m 03$ in *V* (Koen et al. 1999). Only one period is known, so it is likely the fundamental period. A summary of known parameters was given by Rodriguez et al. (2000) in the revised δ -Sct catalog. The photometry by Koen et al. was obtained during 18 hours on two consecutive nights and analyzed together. The authors mentioned that the *V*- and *B*-band phases were statistically identical but hinted that there may be additional low-amplitude frequencies. Koen et al. (1999) pointed out some target confusion in the Geneva photometry catalog (Rufener 1988) that likely came from observing V841 Cen instead of V1034 Cen.

4. Results and discussion

Fig. 2 shows the entire time series V841 Cen minus V1034 Cen for Johnson *V* and *R*. Note again that the comparison star CD-59°5309, one-magnitude fainter than the

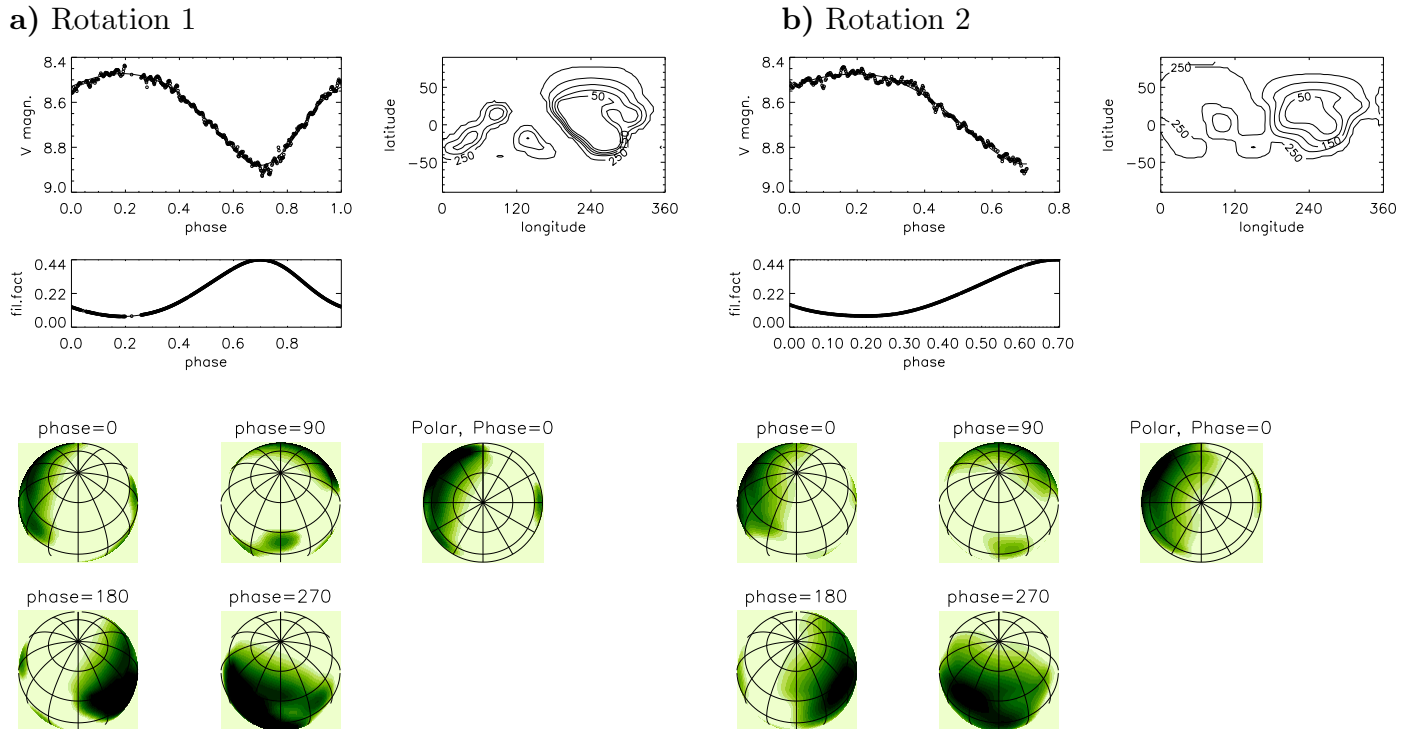


Fig. 6. A spot model for V841 Cen. **a** Stellar rotation #1, **b** Stellar rotation #2. Each panel shows the fit to the V-band data (top left), the spot-filling factor in % per hemisphere as a function of rotational phase (middle), a contour spot map in Mercator projection (top right), and maps of the stellar surface in spherical and flattened pole-on view (entitled polar) in the lower panels. Note that phase zero coincides with our first data point.

two target stars, could not be used as such due to a CCD-controller problem. Therefore, our first step was to separate the light variability of the two stars. Fortunately, this can be done quite accurately because of the star’s significantly different variability periods and amplitudes.

4.1. The rotation period of V841 Cen

Our periodogram analysis for the combined V841 Cen minus V1034 Cen V data prominently shows just the expected single frequency of around six days. We independently apply four different period-search routines to the combined differential data and then examine the pre-whitened output. Phase Dispersion Minimization (PDM, Lafler & Kinman 1965, Stellingwerf 1978) and Lomb-Scargle (LS, Scargle 1982) result in a comparably broad χ^2 minimum and consequently a just moderately-well determined period of 5.881 days and 5.884 days, respectively. The Minimum String Length (MSL, Dworetzky 1983) and the CLEAN algorithm (Roberts et al. 1987) provide a significantly sharper minimum and also give marginally longer periods of 5.8872 days and 5.8854 days, respectively. Just because of consistency reasons we adopt the CLEAN period as the most likely rotation period of V841 Cen with an accuracy based on the rms of the four periods (0.0026 days). Note that an internal error of 10^{-6} days is obtained from the width of its χ^2 minimum via the criterium of Bevington (1969).

The surface rotation is thus synchronized to within 2% of the orbital period and suggestive of an older system, which appears to be somewhat in contradiction with its relatively high lithium abundance. The K subgiant has an upper limit Li abundance that is about a factor 10 below what

is considered to be a lithium-rich star but appears with a higher than normal Li surface abundance (do Nascimento et al. 2003). High degrees of synchronization of the magnetically active component in RS CVn binaries is typical of the vast majority of systems with orbital periods up to 30 days (Fekel & Eitter 1989).

4.2. The pulsation spectrum of V1034 Cen

The base rotational frequency of V841 Cen and up to 6 of its higher-order multiples are identified and subtracted from the combined light curve. The remaining V1034 Cen contribution is shown in Fig. 5a along with the least-squares fit from a total of 41 frequencies of which 24 are ranked significant according to the criterium of Breger (1993), which suggests a 99.9% probability for a peak not to be generated by noise if the obtained amplitude S/N exceeds 4.0. Note that the least-squares fit was obtained from the combined light curve, including the 7 frequencies needed to describe the V841 Cen light curve, but only the pre-whitened output is plotted in Fig. 5a. The final χ^2 achieved was 6.8 mmag, close to the average photometric precision. The periodogram from just the reconstructed V1034-Cen data is shown in Fig. 5b. Using the CLEAN approach, a total of 10 periods appear above a false-alarm probability (FAP) of 10^{-9} with peak-to-valley amplitudes in the range up to 12 mmag. Still 10 more periods appear above a FAP of 10^{-6} with amplitudes below ≈ 6 mmag. Our frequency resolution from the full width at half maximum of the spectral window is 0.062 cycle/d. Frequencies shorter than ≈ 0.2 cycle/d are problematic because these get close to the rotation cycle of the spotted star (0.17 cycle/d) and could be misinterpreted.

E.g., a frequency of 0.145 cycle/d (Table 2) has formally an amplitude of 9.75 mmag and would be highly significant but is judged particularly uncertain because its cycle length of 6.9 days is close to the length of the entire data set and close to the rotation period of V841 Cen. In Table 2 we list all frequencies that we consider significant with respect to the data quality and the periodogram analysis. Note that the original frequency of ≈ 4.2 cycle/day (a period of ≈ 0.2 days) found by Koen et al. (1999) is reconstructed as the strongest peak in our data set in Fig. 5b at 4.20018 cycle/d, which nicely confirms Koen et al.’s initial discovery.

4.3. A spot model for V841 Cen

We employ the new light-curve inversion code of Savanov & Strassmeier (2008). It reconstructs the stellar surface spot configuration from multi-color light curves by using a truncated least-squares estimation of the inverse problem’s objects principal components. Our unknown object, the photospheric spot-filling factor, is a composite of a two temperature contribution; the intensity from the photosphere, I_P , and from cool spots, I_S , weighted by the fraction f of the surface covered with spots, i.e. the spot filling factor. The intensity per pixel reads then

$$I = f \times I_P + (1 - f) \times I_S \quad (1)$$

with $0 < f < 1$. The inversion results in the distribution of the spot filling factor over the visible stellar surface that best fits the data. No assumptions for the shape or for the configuration or total number of spots are made. The stellar astrophysical input includes band-pass fluxes calculated from atmospheric models from Kurucz (2000).

An effective temperature for V841 Cen of 4390 K was listed in Barrado y Navascués et al. (1998) who based it on $V - I$ and $R - I$ indices. Note that just $B - V$ alone would suggest a 300-K higher temperature of $\approx 4,700$ K based on, e.g. Flower (1996). Karatas et al. (2004) gave a spectroscopic parallax that places V841 Cen at a distance of 63_{-13}^{+26} pc and thus with an accordingly uncertain luminosity of $\approx 2.3 L_\odot$ (no *Hipparcos* parallax is available). Our best rotation period of 5.8854 days and the projected rotational velocity of $10 \pm 1 \text{ km s}^{-1}$ from De Medeiros et al. (1997) determine together the lower limit of the stellar radius to $R \sin i = 1.16 \pm 0.12 R_\odot$. Assuming the luminosity based on the spectroscopic parallax and the Stefan-Boltzmann law we obtain a matching radius only with inclinations of as low as 30° and 26° for effective temperatures of 4700 K and 4400 K, respectively. Cutispoto (1998b) favored a K3(V-IV) spectral type from the observed long-term *UBVRI* colors which leads to a slightly higher inclination of $\approx 40^\circ$ ($\pm 10^\circ$) and $T_{\text{eff}} = 4500$ K. These are the values we adopt for the spot modelling. A generally low inclination is also in agreement with the low mass function of $f(m) = 0.025$ from the orbit by Collier (1982a) and the fact that we do not see eclipses nor a secondary star in any of the published spectra (e.g. Randich et al. 1993). In any case, the numerical light-curve simulations by Savanov & Strassmeier (2008) showed that a change of the inclination angle of even $\pm 15^\circ$ just marginally altered the light-curve solution.

Due to the continuous time coverage we do not need to convert the data into phase space but separate into first and second rotation based on a period of 5.8854 days. Five consecutive data points were always averaged. Fig. 6 shows

the results for the consecutive 1.7 stellar rotations, dubbed “rotation 1” and “rotation 2”. A huge spot covering up to 44% of the visible hemisphere is required to fit the deep $0^{\text{m}}4$ photometric minimum. A second, smaller spot with $\approx 10\%$ filling factor at a longitude of $\approx 100^\circ$ (phase $0^{\text{e}}28$) located in the adjacent hemisphere is needed to fit the broad shape of the light curve near maximum light. Note that our inversion algorithm converges with a χ^2 of the fit that is always the (average) χ^2 of the data. Despite the low inclination of the rotational axis, and the therefore pronounced pole-on view, the inversion reconstructs both spots at low latitudes rather than at the poles. This is due to the deep and relatively sharp photometric minimum that excludes a polar, permanently-in-view location.

A spot coverage of 44% of the visible hemisphere is among the largest measured values for active stars, and is by chance the same value as determined for the largest spot ever recorded with the Doppler-Imaging technique (for XX Tri, a K-giant in a 24-day RS CVn binary; Strassmeier 1999). However, spot sizes obtained from photometry depend on the spot temperature. The full $\Delta(V - R)$ amplitude in our data is $0^{\text{m}}090 \pm 0.004$, becoming redder during minimum brightness and bluer during maximum brightness. Our inversion code resolves this with a most likely spot temperature of 3750 K. Its error is obtained from the numerical simulations in Savanov & Strassmeier (2008) that suggested that f increases up to 30% if $\Delta T = T_P - T_S$ is lowered by 250 K. We conclude that $f = 44 \pm 3\%$ and $\Delta T = 750 \pm 100$ K are the most likely spot parameters for V841 Cen at the time of our observations.

Because the orbit determination is almost 30 years old and had a just modestly precise period, it is impossible to identify the exact orbital phase for the time of our data in 2007. Therefore, no statement can be made regarding the location of the largest spot with respect to the orbital frame. However, this would be needed to interpret the magnetic-flux emergence in such a binary because the proximity of the companion star breaks the rotational symmetry and cause a non-uniform surface flux distribution (e.g. Holzwarth 2004).

5. Conclusions and outlook

We presented 243 continuous hours of optical photometry from Antarctica with a duty cycle of 98% and a cadence of 155 seconds. A 3 mmag rms precision in V over 2.4 hours with the 25-cm sIRAIT telescope was achieved for the two bright $8^{\text{m}}5$ target stars. This is a factor 3–4 better than what we had obtained with the 25-cm T1 automatic photoelectric telescope (APT) at Fairborn Observatory in southern Arizona (Strassmeier et al. 1997, Henry 1995). Most likely this is attributed to scintillation noise smaller by a factor 3–4 compared to temperate observing sites, as reported by Kenyon et al. (2006). We conclude that high-precision continuous photometry within the turbulent ground layer just one meter above ground is feasible at Dome C, even with low-cost, partly commercial components. The main problems we had encountered with sIRAIT in its first winterover were all due to the quality of the equipment rather than with the harsh Antarctic environment. This makes us strongly believe that our proposed 2×60 -cm, more optimized and robust, photometric facility ICE-T (Strassmeier et al. 2007b) as well as the intermediate-step 40cm *a-step* experiment (Fressin et al.

2007) are well suited for a site like Dome C and could, for some favorable cases, even challenge photometry from space.

Acknowledgements. The field activities and the results at Dome C benefit from the support of the French and Italian polar agencies IPEV and PNRA in the framework of the Concordia station programme. We thank the AstroConcordia astronomers D. Mékarnia and F. Jeanneaux for their support during the winterover. Heidi Korhonen kindly provided the scintillation noise values for temperate sites. We thank an anonymous referee for several helpful suggestions that improved the paper. German participation in sIRAiT was financed by AIP through the State of Brandenburg and the federal Ministry of Education and Research and supported by the German polar agency AWI. Discussions with Michel Breger on the significance of pulsation frequencies is also appreciated. Finally, we acknowledge support from the European Community's Sixth Framework Programme under contract number RICA-026150 (ARENA).

References

- Agabi, A., Aristidi, E., Azouit, M., Fossat, E., Martin, F., Sadibekova, T., Vernin, J., Ziad, A. 2006, *PASP* 118, 344
- Bertin, E., Arnouts, S. 1996, *A&AS* 117, 393
- Bevington, P. R. 1969, *Data Reduction and Error Analysis for the Physical Sciences*, McGraw-Hill, New York
- Briguglio, R. 2008, PhD thesis, Univ. of Perugia
- Barrado y Navascués, D., De Castro, E., Fernández-Figueroa, M., Cornide, M., García López, R. J. 1998, *A&A* 337, 739
- Bopp, B. W., Africano, J., Quigley, R. 1986, *AJ* 92, 1409
- Breger, M., Stich, J., Garrido, R., et al. 1993, *A&A* 271, 482
- Catala, C., Foing, B. H., Baudrand, J. et al. 1993, *A&A* 275, 245
- Collier, A. C. 1982a, Ph.D. Thesis, University of Canterbury, New Zealand
- Collier, A. C. 1982b, *Southern Stars* 30, 177
- Cutispoto, G. 1990, *A&AS* 84, 397
- Cutispoto, G. 1993, *A&AS* 102, 655
- Cutispoto, G. 1996, *A&AS* 119, 281
- Cutispoto, G. 1998a, *A&AS* 127, 207
- Cutispoto, G. 1998b, *A&AS* 131, 321
- Dempsey, R. C., Linsky, J. E., Fleming, T., Schmitt, J. H. M. M. 1993, *ApJS* 86, 599
- Deeg, H. J., Belmonte, J. A., Alonso, R., Horne, K., Alsubai, K., Doyle, L. R. 2005, in Giard, M. et al. (eds.), *Dome C, Astronomy, and Astrophysics Meeting*, EDP Publ. Ser. 14, p.303
- De Medeiros, J. R., Do Nascimento, J. D., Mayor, M. 1997, *A&A* 317, 701
- Distefano, E., Messina, S., Cutispoto, G., Parihar, P. S., Comparato, M., Busá, I., Lanza, A. F., Lanzafame, A. C., Pagano, I., Strassmeier, K. G. 2007, in Epchtein, N. et al. (eds.), *Large Astronomical Infrastructures at Concordia, Roscoff, EDP sciences, EAS Publ. Ser. Vol. 25*, p.165
- Do Nascimento, J. R., Canto Martins, B. L., Melo, C. H. F., Porto Mello, G., De Medeiros, J. R. 2003, *A&A* 405, 723
- Dworetzky, M. M. 1983, *MNRAS* 203, 917
- ESA 1997, *The Hipparcos and Tycho Catalogues*, ESA SP-1200
- Fekel, F. C., Eitter, J. J. 1989, *AJ* 97, 1139
- Flower, P. J. 1996, *ApJ* 469, 355
- Fossat, E. 2005, in Giard, M. et al. (eds.), *Dome C, Astronomy, and Astrophysics Meeting*, EDP Publ. Ser. 14, p.121
- Fressin, F., Guillot, T., Schmider, F.-X. et al. 2007, in Epchtein, N., et al. (eds.), *Large Astronomical Infrastructures at Concordia, Roscoff, EDP sciences, EAS Publ. Ser. Vol. 25*, p.225
- Harvey, J. W., Hill, F., Hubbard, R. et al. 1996, *Science* 272, 1284
- Henry, G. W. 1995, in Henry, G.W. & J. A. Eaton (eds.), *Robotic Telescopes: Current Capabilities, Present Developments, and Future Prospects for Automated Astronomy*, ASP Conf. Ser. Vol. 79, p.37
- Holzwarth, V. 2004, *AN* 325, 408
- Houk, N., Cowley, A. 1975, *Michigan Catalog*, Vol. 1, Ann Arbor: Astron. Dept.
- Innis, J. L., Coates, D. W. 2008, *IBVS* 5838
- Innis, J. L., Thompson, K., Coates, D. W. 1998, *IBVS* 4570
- Janesick, J. 1997, *SPIE* 3019, 70
- Karatas, Y., Bilir, S., Eker, Z., Demircan, O. 2004, *MNRAS* 349, 1069
- Kenyon, S. L., Lawrence, J., Ashley, M. C. B., Storey, J. W. V., Tokovinin, A., Fossat, E. 2006, *PASP* 118, 924
- Koen, C., Van Rooyen, R., Van Wyk, F., Marang, F. 1999, *MNRAS* 309, 1051
- Kurucz, R. L. 2000, <http://www.cfaku5.harvard.edu>
- Lafler, J., Kinman, T. D. 1965, *ApJS* 11, 216
- Landolt, A. U. 2007, *AJ* 133, 2502
- Lawrence, J. S., Ashley, M. C. B., Tokovinin, A., Travouillon, T. 2004, *Nature* 431, 278
- Mekkadén, M. V., Geyer, E. H. 1988, *A&A* 195, 214
- Mitrou, C. K., Mathioudakis, M., Doyle, J. G., Antonopoulou, E. 1997, *A&A* 317, 776
- Moore, A., Aristidi, E., Ashley, M., et al. 2007, in Epchtein, N., et al. (eds.), *Large Astronomical Infrastructures at Concordia, Roscoff, EDP sciences, EAS Publ. Ser. Vol. 25*, p.35
- Nather, R. E., Winget, D. E., Clemens, J. C., Hansen, C. J., Hine, B. P. 1990, *ApJ* 361, 309
- Newberry, M. V. 1991, *PASP* 103, 122
- Pont, F., Bouchy, F. 2005, in Giard, M. et al. (eds.), *Dome C, Astronomy, and Astrophysics Meeting*, EDP Publ. Ser. 14, p.155
- Randich, S., Gratton, R., Pallavicini, R. 1993, *A&A* 273, 194
- Roberts, D. H., Lehár, J., Dreher, J. W. 1987, *AJ* 93, 968
- Rodriguez, E., Lopez-Gonzalez, M. J., Lopez de Coca, P. 2000, *A&AS* 144, 469
- Rufener, F. 1988, *Catalogue of Stars measured in the Geneva Observatory Photometric System*, 4th ed., Geneva Obs., Sauverny
- Savanov, I. S., Strassmeier, K. G. 2008, *AN* 329, 364
- Schlegel, J. D. 1982, *ApJ* 263, 835
- Schild, R. E., Garrison, R. F., Hiltner, W. A. 1983, *ApJS* 51, 321
- Slee, O. B., Stewart, R. T. 1989, *MNRAS* 236, 129
- Stellingwerf, R. F. 1978, *ApJ* 224, 953
- Strassmeier, K. G. 1999, *A&A* 347, 225
- Strassmeier, K. G. 2007, in Epchtein, N. et al. (eds.), *Large Astronomical Infrastructures at Concordia, Roscoff, EDP sciences, EAS Publ. Ser. Vol. 25*, p.233
- Strassmeier, K. G., Agabi, K., Agnoletto, L., et al. 2007a, *AN* 328, 451
- Strassmeier, K. G., Andersen, M., Granzer, T., Korhonen, H., Herber, A., Cutispoto, G., Rafanelli, P., Horne, K. 2007b, in C. Afonso et al. (eds.), *Transiting Extrasolar Planets Workshop*, ASP 366, p.332
- Strassmeier, K. G., Bartus, J., Cutispoto, G., Rodonó, M. 1997, *A&AS* 125, 11
- Strassmeier, K. G., Hall, D. S., Fekel, F. C., Scheck, M. 1993, *A&AS* 100, 173
- Strassmeier, K. G., Oláh, K. 2004, *ESA SP-583*, 149
- Strassmeier, K. G., Paunzen, E., North, P. 1994, *IBVS* 4066
- Tosti, G., Busso, M., Nucciarelli, G., et al. 2006, *SPIE* 6267, 47
- Udalski, A., Geyer, E. H. 1984, *IBVS* 2594
- Vernin, J., Agabi, K., Aristidi, E., et al. 2007, in Epchtein, N., et al. (eds.), *Large Astronomical Infrastructures at Concordia, Roscoff, EDP sciences, EAS Publ. Ser. Vol. 25*, p.23
- Walker, G. A. H., Croll, B., Kuschnig, R., et al. 2007, *ApJ* 659, 1611
- Weiler, E. J., Stencel, R. E. 1979, *AJ* 84, 1372
- Zacharias, N., Monet, D. G., Levine, S. E., Urban, S. E., Gaume, R., Wycoff, G. L. 2005, *Bulletin of the American Astronomical Society*, Vol. 36, p.1418